Advancement in Scientific and Engineering Research
Vol. 4(1), pp. 1-16, May 2019
doi: 10.33495/aser_v4i1.19.101
ISSN: 2384-7336
Research Paper

Heat transfer and fluid dynamics on inclined smooth and rough surfaces by the application of the similarity and integral methods

Élcio Nogueira[1]* • Marcus V. F. Soares[2] • Luiz Cláudio Pimentel[3]

[1]Faculty of Technology of the State University of Rio de Janeiro - FAT/UERJ, Brazil.
[2]Engineering Company - Engevale, Brazil.
[3]Institute of Geosciences of the Federal University of Rio de Janeiro - IGEO/UFRJ, Brazil.

*Corresponding author. E-mail: elcionogueira@hotmail.com

Accepted 29th March, 2019.

Abstract. The main objective of the analysis is to review and discuss the principles of the similarity method applied to the boundary layer on inclined surfaces, in laminar regime, and that can be extended to a turbulent regime. The emphasis applies to theoretical aspects related to the concept of similarity, but theoretical results were obtained in order to compare with empirical expressions and experimental results. Results are obtained for the hydrodynamic and thermal fields, such as coefficient of friction and Stanton number, as a function of the pressure gradient parameter and the Prandtl number. The fourth order Runge-Kutta method is applied, starting from the expansion in power series as the first approximation for the mathematical solution of hydrodynamic and thermal problems, in laminar regime. The Integral Method is applied to obtain an approximate solution for the flow in turbulent regime, by similarity variables method. Numerical and graphical results are presented in sufficient numbers to emphasize the consistency of the model developed in the determination of parameters related to thermal and hydrodynamic boundary layers on smooth and rough surfaces.

Keywords: Similarity method, fourth order Runge Kutta Method, hydrodynamic boundary layer; thermal boundary layer.

INTRODUCTION

At the beginning of the twentieth century, important developments occurred in the hydrodynamic theory of the flows in the bodies, which provided explanations for the observed discrepancies between the theory of hydraulic and equations of Euler for an ideal fluid. Navier-Stokes equations were already available, but the degree of difficulty imposed for complete solution of the equations, even for simple problems, and low viscosity fluids such as air and water, has not provided a satisfactory solution to the needs of the moment. In 1904 Prandtl developed the concept of boundary layer, demonstrated that the flow around a body is divided into two regions: a thin layer close to the body, where the viscous tensions are preponderant, and an outer region where viscous forces can be neglected. Through this "artifice", simpler equations, derived from the Navier-Stokes equations could be deduced and resolved with relative ease for flat plate flow Blasius (1908), Hager (2003) and sloping surfaces Falkner and Skan (1930, 1931) in laminar regime.

The boundary-layer equations made it possible to rapidly advance the theory of fluid mechanics and its application to airfoils; which is an important application for aircraft design. The boundary layer theory has also brought advances in the solution of problems associated with the heat transfer around bodies. The classical

mathematical method chosen to solve this class of problems is called the "Similarity Method".

The similarity method makes it possible to transform a nonlinear third order partial differential equation into an ordinary differential equation. It is now considered that the main aspects of the similarity theory have already been clarified. Extensions of the theory were applied to the turbulent regime, and the boundary layer concept associated with the similarity method continues to be used as a basis for more complex problems than those analyzed by Blasius and Falkner and Scan. These are extensively published in traditional textbooks. However, due to the complexity of the turbulent flows, a complete theory, based on the principle of similarity, still does not exist and research continues to be carried out in this area (Abbasi *et al*., 2014; Bhattacharyya *et al*., 2016; Bognar and Hriczó, 2011; Castilho, 1997; Myers, 2010; Rahman, 2011; Stemmer, 2010).

Analytical methods of solution of partial nonlinear differential equations, based on stream function and similarity method are being applied to solve numerous engineering problems.

Buoyancy-driven, incompressible, two-dimensional flow of a micropolar fluid inside an inclined porous cavity in the presence of magnetic field is investigated by Nazeer *et al*. (2017). The nonlinear partial differential equations are solved by employing a robust Galerkin finite element scheme. The code is validated and benchmarked with the previous numerical data available in the literature.

Sheikhzadeh and Abbaszadeh (2018) determined the solutions for the momentum and energy equations of laminar flow of a non-Newtonian fluid in an axisymmetric porous channel using the least squares and Galerkin methods. The numerical solution is conducted using fourth order Runge-Kutta method. With comparing the results obtained from the analytical and numerical methods, a good adaptation can be seen between them. It can also be observed that the results of the Galerkin method have further conformity with the numerical results and the Galerkin method is simpler than the least square method and requires fewer computations.

Ali *et al*. (2019) performed a numerical study for the mixed convection flow inside a triangular cavity. The rheological behavior of the fluid inside the cavity is modeled through the constitutive bi-viscosity equation. The governing nonlinear partial differential equations are discretized using Galerkin finite element method and pressure is eliminated through the penalty method. The computations are presented graphically for a wide range of the bi-viscosity parameter, thermal radiation parameter, Hartman number, Grashof number, Reynolds number, heat generation/absorption parameter and Prandtl number.

Rabari *et al*. (2017) present an analytical study on the blood flow containing nanoparticles through porous blood vessels, in the presence of magnetic field, using the Homotopy Perturbation Method (HPM). The viscosity of nanoparticles is determined by Constant, Reynolds' and Vogel's models. It is observed that velocity reduces at higher values of magnetic field intensity.

The problem of the steady, incompressible, three-dimensional stagnation point flow of a micropolar fluid over an off centered infinite rotating disk in a porous medium is studied Khan *et al*. (2017). Injection/suction is applied uniformly throughout the surface of porous disk. The Darcy's resistance for the micropolar fluid is also formulated. The partial differential equations are converted into the set of ordinary differential equation by utilizing the suitable transformation. The system of equations is analytically solved by the means of a non-perturbative technique, homotopy analysis method (HAM). The influence of rotational parameter, material parameter, spin gradient viscosity parameter, micro-inertia density parameter, porosity parameter and suction/injection parameter on velocity functions is presented in graphical form and discussed in detail. Verification of the solutions is made by a numerical comparison with the previous study.

Aziz *et al*. (2018) analyzes the heat transfer of a thin film flow on an unsteady stretching sheet in nanofluids. Three different types of nanoparticles are considered; copper Cu, alumina Al_2O_3 and titania TiO_2 with water as the base fluid. The governing equations are simplified using similarity transformations. The resulting coupled nonlinear differential equations are solved by the Homotopy Analysis Method (HAM). The analytical series solutions are presented and the numerical results obtained are tabulated. In particular, it shows that the heat transfer rate decreases when nanoparticles volume fraction increases.

Combined influences of thermal radiation, inclined magnetic field and temperature-dependent internal heat generation on unsteady two-dimensional flow and heat transfer analysis of dissipative Casson-Carreau nanofluid over a stretching sheet embedded in a porous medium is investigated by Sobamowo *et al*. (2018). Similarity transformations are used to reduce the developed systems of governing partial differential equations to nonlinear third and second orders ordinary differential equations which are solved using finite element method. In the study, kerosene is used as the base fluid which is embedded with the silver (Ag) and copper (Cu) nanoparticles. Also, effects of other pertinent parameters on the flow and heat transfer characteristics of the Casson-Carreau nanofluids are investigated and discussed.

In this work, the aspects related to laminar regime are associated, mainly, with the works of Evans (1968) and the aspects associated to the turbulent regime, smooth and rough surface, are related to the works of Kays *et al*. (1969).

The results obtained enable simplifications to be used in numerous practical situations, such as modeling for determination of micro meteorological parameters, as

recommended in Monin-Obukov's theory of similarity Stull (1988).

Objectives

The main objective is to review and discuss the principles of the method of similarity applied to boundary layer on sloped, smooth and rough surfaces, laminar and turbulent regimes. Emphasis applies to theoretical aspects related to the concept of similarity and integral method, but results were obtained with the aim of comparing with empirical expressions and experimental results.

A secondary objective is to present the main aspects of the problem analyzed by Falkner and Skan, focusing on the similarity method, which can be extended, as already stated, to more complex problems of flow and heat transfer in turbulent regime.

For comparison purposes, the problem of flux flow and heat transfer in turbulent regime in boundary layer on inclined surfaces, using velocity profile with an exponent one-seven (1/7), is applied as an extension of the solution with zero gradient of pressure, presented by Kays and Crawford (1983) and Nogueira and Soares (2018).

METHODOLOGY

The aspects related to laminar regime are based on the deep study carried out by Evans (1968), and in turbulent regime the text of Kays and Crawford (1966).

It is assumed that there is no mass transfer through the surface (without surface perspiration effect) and that the perpendicular component of velocity is zero. In addition, the velocity component parallel to the surface is also zero, a condition called "no slip on the wall" in the specialized literature. All the presented solutions and results assume constant properties, unaffected by the variation of temperature, and the velocities are sufficiently low so that the viscous dissipation term can be neglected.

The basic equations for boundary layer similarity conditions are widely discussed Schlichting (1968); Evans (1968), Kays and Crawford (1983), Silva Freire (1990), and only essential details for the understanding of the arguments are presented in this work. Details on flat plate flow are discussed by Nogueira and Soares (2018).

There are in the literature many ways of specifying the existence of similar solutions for the laminar boundary layer equations. The main characteristic associated with the concept of boundary layer similarity is that the undisturbed velocity distribution of the potential flow must satisfy the following expression, which follows the original suggestion of Falkner and Scan (1931):

$$U(x) = Cx^m \tag{1}$$

where C is the value of U (x) where x is unitary, and the value of m depends on the pressure gradient in the main direction of the flow. However, according to Spalding and Pun (1962), it is convenient to impose that U (x) satisfies the following equation:

$$\frac{dU}{dx} = CU^{\frac{2(\beta-1)}{\beta}} \tag{2}$$

where β is a parameter that is associated with the pressure gradient in the direction of the main flow.

The potential theory, applied around an angle wedge βπ/2 Evans (1988), satisfies Equation 1, above, where:

$$m = \frac{\beta}{(2-\beta)} \tag{3}$$

and,

$$\frac{1}{\beta}\frac{dU}{dx} = \frac{U}{x}\frac{1}{(2-\beta)} \tag{4}$$

However:

$$\frac{dp}{dx} = -\rho U\frac{dU}{dx} \tag{5}$$

The specification of U (x) is equivalent to specifying the pressure gradient, which is a function of β:

$$\frac{dp}{dx} = -\rho U\frac{\beta}{(2-\beta)}\frac{U}{x} \tag{6}$$

The parameter β, as can be seen, depends only on the velocity distribution in the external region to the boundary layer, the variable x along the surface and the pressure gradient.

We are interested in the flow conditions where -0.2 ≤ β ≤ 1.0, representing the limits of the boundary conditions for the pressure gradient parameter between the boundary layer detachment β=-0.2, and the two-dimensional stagnation flow β=1.0, in the laminar regime (Figure 1).

The differential equation governing the velocity distribution at a similar boundary layer for laminar regime within the range of the already established pressure gradient parameter β is given by Schlichting (1968); Evans (1968), Kays and Crawford (1983), Silva Freire (1990):

$$f''' + f.f'' + \beta.\left(1 - f'^2\right) = 0 \tag{7}$$

with the following boundary conditions:

$\eta = 0, \quad f = f' = 0$ 7.1
$\eta \to \infty, \quad f' \to 1.0$ 7.2

where f and η are defined by:

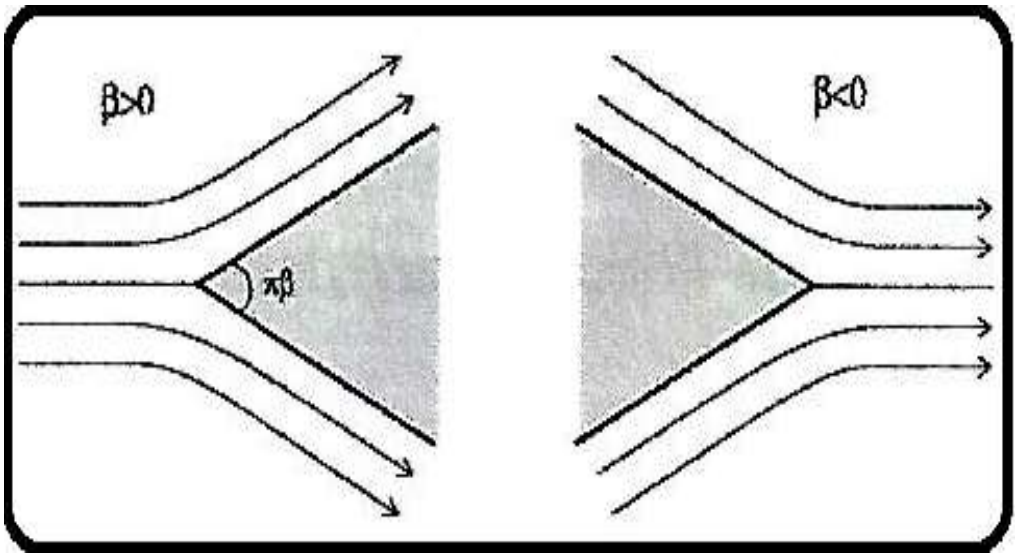

Figure 1. Flow on an inclined surface of angle πβ.

$$\eta = \frac{y}{x}\frac{(\frac{Ux}{\upsilon})^{1/2}}{\sqrt{2-\beta}} \quad e \quad f = \frac{\psi/\upsilon}{(\frac{Ux}{\upsilon})\sqrt{2-\beta}} \tag{8}$$

where x and y are, respectively, the primitive coordinates along the surface and perpendicular to it.

Choosing the coordinate η as a function of y / x, which is very small, except at x = 0, by the square root of the Reynolds number, $Re_x = (\frac{Ux}{\upsilon})^{1/2}$, which is very large, we impose y/x is small, but η is not.

From the definitions of η and f, we have expressions for the components of dimensionless velocities:

$$u = U\frac{df}{d\eta} \quad e \quad v = -\left(\frac{\upsilon}{\beta}\frac{dU}{dx}\right)^{\frac{1}{2}}[f + (\beta-1)\eta\frac{df}{d\eta} \tag{9}$$

The last boundary condition, Equation 7.2, means that as η grows $f' = u/U$ should approach the unit without exceeding it. The value of η, in this case, is called η_∞, for a given value of β.

Due to the difficulty in solving the above boundary condition problem with reasonable precision, we apply the 4th order Runge Kutta Method (Tannehill *et al*., 1997), with initial value of f''(0) given after application of the Power Series Method.

The approximate solution by the power series method with the Shooting Method (Tannehill *et al*., 1997; Oderin, 2014), as an approximation procedure for the velocity profile is obtained by assuming that the function f (η) satisfies the following expansion in series:

$$f(\eta) = C_2\frac{\eta^2}{2!} + C_5\frac{\eta^5}{5!} + C_6\frac{\eta^6}{6!} \ldots + C_n\frac{\eta^n}{n!} \tag{10}$$

With the following recurrence rule:

$$C_{n+3} = -n!\left[\frac{1}{1!\,(n-1!)}(\beta.C_2.C_n) + \frac{1}{2!\,(n-2!)}(C_2.C_n + \beta.C_3.C_{n-1}) + \frac{1}{3!\,(n-3!)}(C_3.C_{n-1}) + \frac{1}{4!\,(n-4!)}(C_5.C_{n-3})\right] \tag{11}$$

for n≥4.

$$C_3 = -\beta\,;\; C_5 = -2\left(\beta+\frac{1}{2}\right)C_2{}^2 \quad e \quad C_6 = 6\beta\left(\beta+\frac{1}{2}\right)C_2 \tag{12}$$

The term C_2 corresponds to f "(0), that is:

$$C_2 = f''(0) \tag{13}$$

Through Shooting Method (Tannehill *et al*., 1997; Oderinu, 2014), or other approach method, as the "Bisection Method", we can obtain the value of C_2, with the desired approximation. However, the approximation method through the series solution is slow, in order to obtain the necessary solution for our purposes. In this sense, we apply the fourth Runge-Kutta method (Tannehill *et al*., 1997), with initial value for f " (0) from the expansion in power series. As the Runge-Kutta method is a high-precision numerical method, coupled with the Newton-Raphson method, the final solution for the velocity field in the hydrodynamic boundary layer is obtained in less time than necessary for the series

solution, with the same precision.

The energy equation for determining the dimensionless temperature field is given by:

$$\frac{d}{d\eta}(\theta') + Pr.f.\theta' = 0 \qquad (14)$$

The temperature profile shall satisfy the following contour conditions for the specified surface temperature:

$\eta = 0, \quad \theta = 0$ 14.1
$\eta \to \infty, \quad \theta \to 1.0$ 14.2

where Pr is the number of Prandtl, and

$$\theta = \frac{T - T_W}{T_\infty - T_W} \qquad (15)$$

It is assumed that T_∞, temperature outside the boundary layer, is not affected by the heat rate removed outside of the boundary layer. The value of T_W corresponds to the surface temperature (reference!).

The energy equation, Equation 14, is linear and less complex than the velocity field equation. However, it strongly depends on the solution of the velocity profile, since f appears explicitly in the second term. Therefore, the greater the precision in the solution of *f*, the better the solution in θ.

The Runge-Kutta method is used for solution of the temperature field, but it is observed that the limit value for η, $\eta \to \infty$, is not necessarily the same as that obtained for the velocity field, for a given β. As an alternative, in terms of comparison, a second solution is obtained by directly integrating the energy equation Kays and Crawford (1983); Evans (1968):

$$\theta = \theta_0' . \int_0^\eta \exp[-Pr. \int_0^\eta f.d\eta]\, d\eta \qquad (16)$$

$$\theta' = \theta_0' . \exp[-Pr. \int_0^\eta f.d\eta] \qquad (17)$$

where θ_0' 'is the value of the surface temperature derivative:

$$\theta \to 1, \quad \eta \to \infty \qquad \theta_0' = \frac{1}{\int_0^\infty \exp[-Pr. \int_0^\eta f.d\eta]\, d\eta} \qquad (18)$$

However, the application of Equation 18, above, does not provide adequate accuracy to obtain the surface temperature gradient. In this sense, we chose to use Evans's procedure, in θ_0'.

Therefore,

$$(\frac{d\theta}{d\eta})_0 = \frac{3}{E}(\frac{Pr.f_0''}{3!})^{1/3} \qquad (19)$$

Where

$$E = \Gamma\left(\frac{1}{3}\right) + \sum_{q=0}^{\infty} \frac{a_q}{Pr^{\frac{q}{3}}} \qquad (20)$$

Γ is the gamma function:

$$\Gamma\left(\frac{1}{3}\right) = 2.6789385 \qquad (21)$$

Expressions for a_q contains the pressure gradient parameter β, the dimensionless viscous stress on the wall $f''(0)$, and numerical factors derived from the combination of gamma functions and are not presented. The complete procedure for the exact determination is found in Evans (1968). In addition, Equation 19, for determining the temperature gradient at the surface, presents unsatisfactory results as β tends to the flow separation value (β = -0.2). Evans (1968) describes an alternative procedure for this case, but it will not be the subject of discussion in this analysis.

In turbulent regime there are no analytical solutions for the boundary layer equations. An alternative for the determination of turbulent boundary layer parameters is the approximate solution of Von Kármán's equation:

$$\frac{d\delta_2}{dx} = \frac{C_f}{2} = \frac{\tau_w}{\rho U^2} \qquad (22)$$

Even in the zero-pressure gradient, flat plate flow, Von Kármán's equation has more unknowns than equations. Thus, it is necessary to relate the unknowns by specifying a dimensionless velocity profile.

For comparison purposes, in relation to the laminar regime, in this work, values for turbulent flow are determined on smooth and rough inclined surfaces, by means of an approximate theoretical model. Turbulent flow with 1/7 power is used, and experimental results of Schultz-Grunow (1941), Pimenta *et al*. (1975), Schlicthing and Prandtl (1968), and Kays and Crawford (1983).

The theoretical procedure, in this case, corresponds to the one recommended by Kays and Crawford (1983), for flat plate flow, where the conditions of similarity are satisfied. In fact, the valid procedure is used for flat plate, for determination of the profiles of speed and temperature, and generalizes to situations where $\beta \neq 0$, through the concept of the shape factor, H_{12}, and correction formulas obtained by Kays and Crawford (1983).

For the approximate determination of the turbulent velocity profile, associated with the integral equation of momentum, a power law of type 1/7 is very convenient:

$$u^+ = 8.75 y^{+1/7} \qquad (23)$$

The above expression represents the speed profile up to $y^+ = 1500$ a little better than the equation, much used in

algebraic simulations, called "Logarithmic Law in the Wall".

$$u^+ = \frac{u}{\sqrt{\tau_w/\rho}} \qquad e \qquad y^+ = y\frac{\sqrt{\tau_w/\rho}}{\upsilon} \tag{24}$$

If Equations 22 and 23 are valid throughout the boundary layer, and that the thickness δ corresponds to the position where the velocity is equal to U, we have:

$$\frac{U}{\sqrt{\tau_w/\rho}} = 8.75\delta\frac{\sqrt{\tau_w/\rho}}{\upsilon} \tag{25}$$

The displacement, δ_1, and momentum thickness, δ_2, can be evaluated by the following expressions:

$$\delta_1 = \int_0^\infty \left(1 - \frac{u\rho}{U\rho_\infty}\right) dy \tag{26}$$

and

$$\delta_2 = \int_0^\infty \frac{\rho u}{\rho_\infty U}\left(1 - \frac{u}{U}\right) dy \tag{27}$$

The integral equation of the momentum, in similar coordinates, is given by:

$$f''(0) = \frac{1}{\delta_4} = \frac{1}{\upsilon U}\frac{d}{x}(U^2\delta_2) + \frac{\delta_1}{\upsilon}\frac{dU}{dx} \tag{28}$$

or

$$\frac{\delta_2}{\delta_4} = \frac{1}{2}\frac{U(x)}{\upsilon}\frac{d{\delta_2}^2}{dx} + (2 + H_{12})\frac{{\delta_2}^2}{\upsilon}\frac{dU(x)}{dx} \tag{29}$$

where

$$H_{12} = \frac{\delta_1}{\delta_2}\ denominated\ shape\ factor \tag{30}$$

For similar boundary layer, each δ_n is a constant and therefore the shape factor is a constant. It is important to note that Equation 28 is valid for laminar and turbulent regime. The shape factor increases in an adverse pressure field, β <0. For flow in turbulent boundary layer, H increases from 1.29 to null pressure gradient β = 0, to approximately 2.7 in the separation condition $\beta \cong 0.2$ Simpson (1989). For accelerated flow the value of H increases again, as a function of the "tendency to laminar flow" effect, and tends to 1.47 for two-dimensional stagnation flow, β = 1 Smith (1966). The velocity distribution, U (x), must be known prior to the application of the integral momentum equation, Equation 28.

The displacement thickness, δ_1, has the effect of displacing the undisturbed main flow current function with respect to the value it should have for ideal, non-viscous fluid. The momentum thickness, δ_2, is the extent to which the amount of fluid movement in the boundary layer is below what should be for an ideal fluid. The viscous thickness, δ_4, inverse of f "(0), is the measure of the resistance offered for transferring the amount of movement of the main stream to the surface.

There are two predominant regions to be analyzed in a turbulent boundary layer:

1. A predominantly viscous region close to the surface, where viscous stresses and molecular conduction prevail;
2. A completely turbulent region where the amount of movement and heat are transported in rates generally much higher than that of the viscous sublayer.

It is in the viscous sublayer, however, where events associated with turbulence occur and are of greater importance than the fully turbulent region. The viscous forces, largely responsible for the characteristics of the laminar flow, have the effect of restoring the laminar flow in turbulent flow and, otherwise, the inertial forces associated with the local variations of the velocity field have the opposite effect. In fact, inertial forces tend to amplify local disturbances. It is to be expected, therefore, that the stability of the laminar flow is associated with low numbers of Reynolds, ratio between the forces of inertia by the viscous forces. Although instability is an essential feature in the viscous sublayer, the turbulent boundary layer structure adjusts itself, constructing a relatively stable structure with stability characteristics (there is regularity!).

At turbulent flow, along the surface, the laminar sublayer becomes narrow and becomes an increasingly smaller fraction of the entire boundary layer. In essence, the turbulent boundary layer has the property of diffusing the amount of movement, and other properties of the flow, much more rapidly than the simple molecular process.

Equations 26 and 27, together with the integral equation of momentum, Equation 28, can be used to obtain the coefficient of friction in the turbulent boundary layer. Note, however, that the velocity profile is valid for null pressure gradients, that is, β = 0. For situations in which the pressure gradient is different from zero, correction must be made. The expression for the coefficient of friction, β = 0, is given by Kays and Crawford (1983):

$$\frac{Cf}{2} = \frac{0.0594}{2Re_x{}^{1/5}} \quad (31)$$

which can be compared with the experimental equation obtained by Schultz-Grunow (1941):

$$\frac{Cf}{2} = 0.185\left(Log_{10}(Re_x)\right)^{-2.584} \quad (32)$$

In turbulent boundary layer analysis, it is convenient to define some type of similarity. However, the task is not as simple as in laminar boundary layer. In turbulent flow, in a region very close to the surface, it is observed that $u^+ = y^+$ e, logically, the principle of similarity applies. Outside this region and in the explicit coordinate system, the principle generally does not apply. However, there are some classes of turbulent flow that have similarity, even outside the laminar sublayer.

Turbulent boundary layer that has similarity outside the laminar sublayer is called the boundary layer in equilibrium. The equilibrium boundary layer is the one that satisfies the following velocity profile:

$$\frac{u-U}{\sqrt{\frac{\tau_w}{\rho}}} = F\left(\frac{y}{\delta_3}\right) \quad (33)$$

Where

$$\delta_3 = -\int_0^\infty \frac{u-U}{\sqrt{\frac{\tau_w}{\rho}}} dy \quad (34)$$

For laminar boundary layer it was demonstrated that Equation 01 must be satisfied for similarity solutions to exist. In turbulent boundary layer this same type of free-flow velocity profile must be satisfied, so that equilibrium boundary layer occurs, satisfying the similarity principle (Kays and Crawford, 1983).

The turbulent coefficient of friction for the equilibrium boundary layer can be correlated with β through an empirical relation (Kays and Crawford, 1983):

$$\frac{Cf/_2}{\left(Cf/_2\right)_{\beta=0}} = \frac{1}{(1+\frac{\beta}{5})} \quad (35)$$

For turbulent boundary layer, assuming equilibrium boundary layer, the Stanton number is determined for null pressure gradient, β = 0, through the expression (Kays and Crawford, 1983):

$$St_x = \frac{Cf/_2}{\sqrt{Cf/_2}\,(13.2Pr - 10.16) + 0.9} \quad (36)$$

RESULTS AND DISCUSSION

Results were obtained for velocity and temperature profiles, and associated values, such as friction coefficient and Stanton number, as a function of the pressure gradient parameter and Prandtl number. Numerical results were computed using Fortran (1995) language and graphical results were obtained through software Grapher (2004).

Figure 2 presents results for velocity profile, f', and dimensionless viscous stress, f'', for laminar regime in extreme situations, in β=-0.2 and β=1.0, in relation to the results obtained for flat plate, β=0. These conditions, as already pointed out, represent, respectively, the surface boundary layer detachment condition and the two-dimensional stagnation flow condition. It is observed that, for β=-0.2, the viscous stress is equal to zero on the surface, as expected.

In Equation 7, for $\beta = 0$, since $f' = 0$ on the wall, f''' is also zero and, as a consequence, f'' has a maximum value on the wall. For $\beta < 0$ values, f'' also has a maximum value, but the maximum point distances itself from the wall, and the values of f'' on the wall are lower than that of $\beta = 0.0$. In fact, it can be observed that the viscous tension in the wall decreases to negative β values and becomes zero in β near -0.2.

For accelerated flows, $\beta > 0$, the maximum value also occurs on the wall, and these values increase with increasing acceleration of the flow. Since the viscous stress is zero on the wall, where the separation of the flow occurs, f' has a minimum at this point, as can be seen from Figure 2. For accelerated flow, $\beta = 1.0$, a decrease in the displacement thickness, relative to flat plate flow, $\beta = 0.0$, can be observed.

Table 1 present comparisons of results for displacement thickness, δ_1, momentum thickness, δ_2, and the inverse of shape factor, H_{21}, in laminar regime. The consistency of the results obtained can be verified. For highly accelerated flows, better consistency is achieved between models.

Figure 3 presents results for temperature profile and dimensionless temperature gradient in laminar regime and Pr = 1.0. The most important results, which should be emphasized, are the values of the surface temperature gradient, since the integral parameters associated to the temperature field are strongly associated with it. It can be observed that the temperature gradient decreases with lower values of β, ie, the more accelerated the flow, the greater the temperature gradients in the wall. Equivalent to what occurs with the thickness of the hydrodynamic boundary layer, the thermal boundary layer thickness also decreases to higher β values. In addition, another factor to be emphasized, the profile and the temperature gradient depend strongly on the solution of the velocity field, according to Equations 16 and 17.

Figure 4 presents the results of a dimensionless coefficient of friction in the laminar regime determined by:

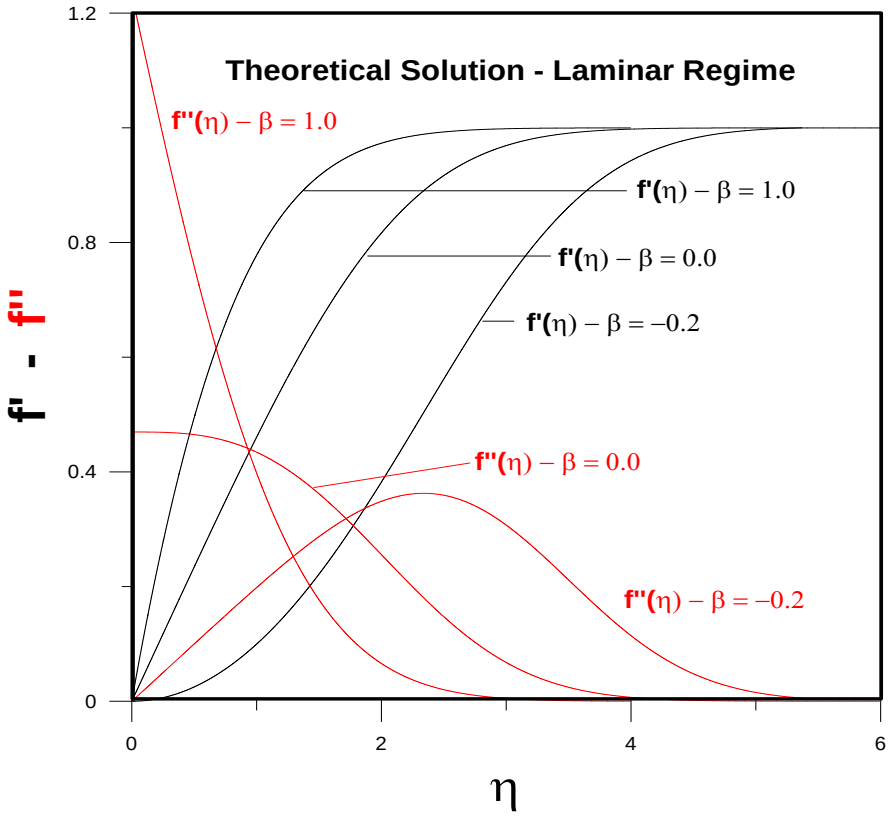

Figure 2. Solutions for dimensionless viscous velocity (f'') and velocity profile (f').

Table 1. Numerical comparisons in laminar regime for the inverse of Shape Factor (H_{21}).

β	Results			Evans (1968)		
	δ_1	δ_2	H_{21}	δ_1	δ_2	H_{21}
-0.2**	2.3587	0.5852	0.2400	2.3588	0.5854	0.2482
-0.019	2.0064	0.5762	0.2834	2.0068	0.5765	0.2873
-0.18	1.8714	0.5673	0.3006	1.8716	0.5677	0.3033
-0.15	1.6468	0.5449	0.3295	1.6470	0.5452	0.3310
-0.12	1.5111	0.5258	0.3472	1.5113	0.5263	0.3482
-0.10	1.4423	0.5147	0.3562	1.4427	0.5150	0.3570
0.0	1.2164	0.4695	0.3856	1.2168	0.4696	0.3859
0.2	0.9839	0.4081	0.4147	0.9842	0.4082	0.4148
0.3	0.9108	0.3856	0.4234	0.9110	0.3857	0.4234
0.4	0.8525	0.3666	0.4300	0.8527	0.3667	0.4301
0.6	0.7639	0.3359	0.4397	0.7640	0.3359	0.4397
0.8	0.6986	0.3119	0.4464	0.6987	0.3118	0.4463
1.0	0.6480	0.2924	0.4514	0.6480	0.2923	0.4513

**β = -0.19883768

$$\frac{Cf}{2} = \frac{f''(0)}{Re_x^{\frac{1}{2}}(2-\beta)^{1/2}} \quad (37)$$

And

$$\left(\frac{Cf}{2}\right)_{empirical} = \frac{[F(\beta)\frac{Cf(\beta=0)}{2}]}{(1+\frac{\beta}{5})} \quad (38)$$

$$\frac{Cf(\beta=0)}{2} = \frac{0.332}{Re_x^{\frac{1}{2}}} \quad (39)$$

where

$$F(\beta) = 0.992436221 + 3.670315583\beta - 2.382778474\beta^2 + 2.203613278\beta^3 \quad (40)$$

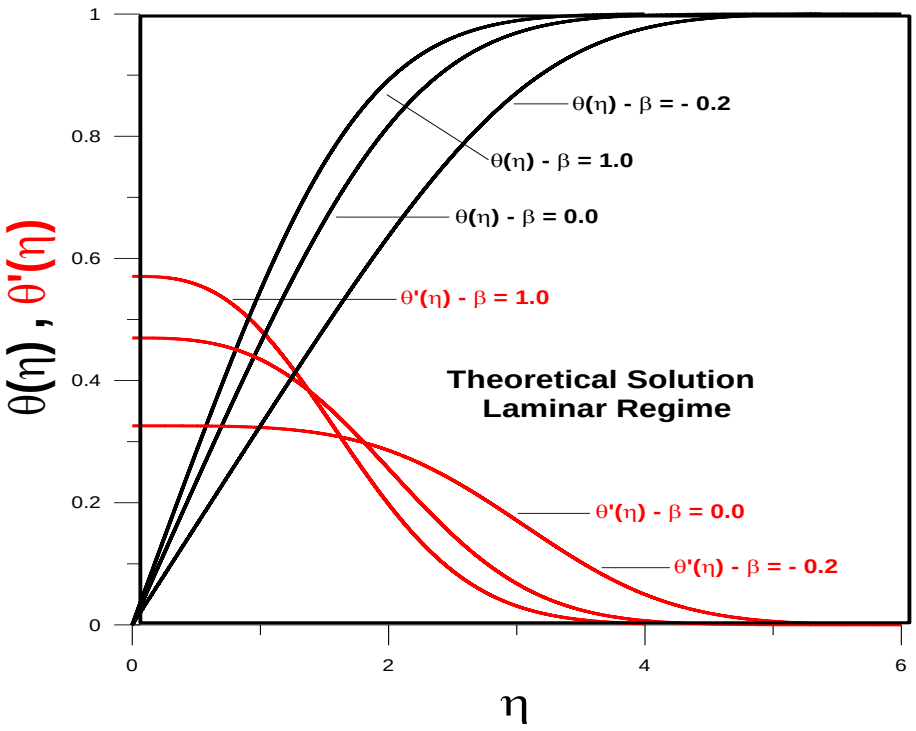

Figure 3. Temperature profile (θ) and dimensionless temperature gradient (θ') for laminar thermal layer (Pr = 1.0).

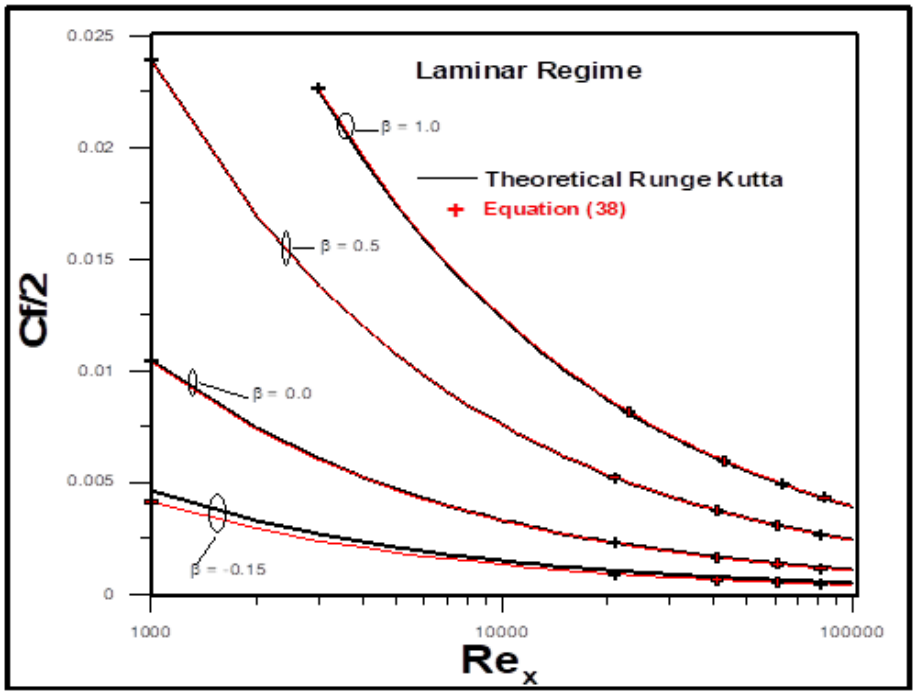

Figure 4. Dimensionless coefficient of friction ($\frac{Cf}{2}$) as a function of the Reynolds number (Re_x) for laminar regime.

$F(\beta)$ is obtained empirically from the data available in Evans (1968).

It is observed that the new empirical solution, Equation 38, is very convenient, since it eliminates the need to

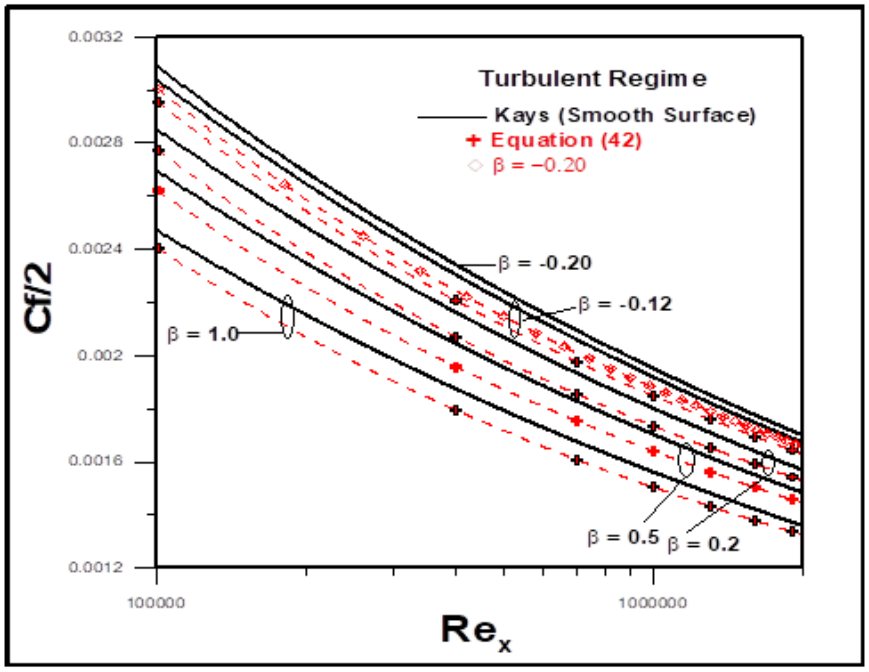

Figure 5. Non-dimensional coefficient of friction $(\frac{Cf}{2})$ as a function of Reynolds number (Re_{x}) for turbulent regime on smooth surface.

solve the hydrodynamic boundary layer equation to obtain the coefficient of friction for the entire range of β. This is one of more significant and important result presented in this work, since the results differ significantly only for values of β <-0.15, and low Reynolds number values along the surface.

Figure 5 shows the results obtained for the dimensionless friction coefficient for turbulent regime on smooth surface. The highlight corresponds to the Schultz-Grunow (1941) modified solution. The analytical solution, Equation 35, and Schultz-Grunow's empirical equation, Equation 42, associated with the modification proposed by Kays and Crawford (1993), for pressure gradient flows within the range analyzed in this work, -0.2 < β < 1.0, are in good agreement. It is, therefore, a result compatible with that presented in Figure 4, since the solution eliminates the need to solve the system of equations for velocity field where β is different from zero.

$$\frac{Cf}{2} = \frac{0.0594}{2Re_x{}^{1/5} * (1 + \frac{\beta}{5})} \tag{41}$$

$$(\frac{Cf}{2})_{Exp} = \left[0.185\left(Log_{10}(Re_x)\right)^{-2.584}\right] / (1 + \frac{\beta}{5}) \tag{42}$$

All previous discussion assumes boundary layer for smooth surface. The effect of roughness on the turbulent boundary layer occurs primarily close to the surface, and this leads to the definition of a rough Reynolds number:

$$\mathrm{Re_k} = \frac{\mathrm{u_\tau k_s}}{\vartheta} \tag{43}$$

where k_s is the absolute roughness.

Figure 6 shows the comparison between valid results for smooth and rough surfaces, for any range of values of the pressure coefficient previously defined, 0.2<β<1.0.

The characteristics of the hydrodynamic and thermal boundary layer are controlled by important parameters such as speed and temperature, shape and surface conditions. Surface conditions require special attention where roughness is an inherent characteristic. Roughness usually increases the friction resistance and the heat transfer coefficient for a same Reynolds number, relative to the smooth surfaces. In fact, the roughness produces higher values for the friction factor and Stanton number, which result in speed and temperature deficits at the relative long distance of the surface when compared to the smooth surface.

For $\mathrm{Re_k}$ > 65 we have what is called the regime for a completely rough surface or even a completely rough flow Pimenta *et al*. (1975). A completely rough regime is what is considered in this analysis and, for all intents and purposes, we have $\mathrm{Re_k}$=70. It can be shown that the friction coefficient, for a completely rough regime, can be obtained by the following expression, where the correction factor for the pressure gradient effect is

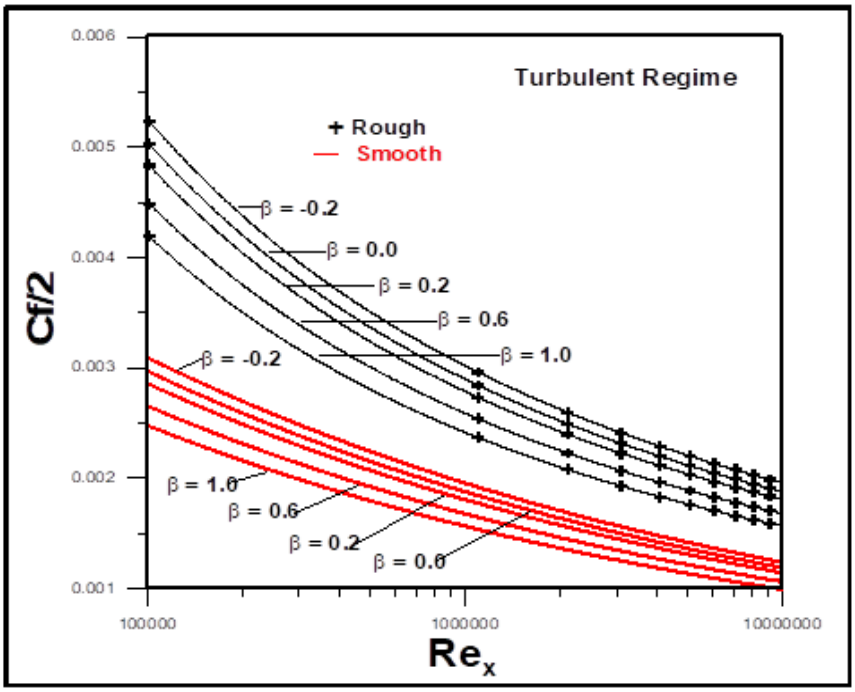

Figure 6. Comparison for dimensionless friction coefficient ($\frac{Cf}{2}$) between smooth and rough surfaces in turbulent regime.

introduced, according to the empirical proposal of Kays and Crawford (1983):

$$(\frac{Cf}{2})_{rug} = \frac{0.168}{\left[\ln\left(\frac{32.1x}{Re_x^{\frac{1}{5}}k_s}\right)\right]^2 (1+\frac{\beta}{5})} \quad (44)$$

The Stanton number, by definition, is obtained from the expression below:

$$St_x = \frac{Nu_x}{\mathrm{Pr}.Re_x} \quad (45)$$

For laminar regime

$$Nu_x = \frac{(\frac{d\theta}{d\eta})_0 \sqrt{\frac{Re_x}{2}}}{(2-\beta)^{1/2}} \quad (46)$$

In any situation, laminar or turbulent regime, for constant surface temperature and constant free-flow velocity, the Stanton number can be expressed in the form:

$$St = CRe_x^{-n} \quad (47)$$

In turbulent regime, zero pressure gradient, smooth surface, Kays and Crawford present the following equation, which fits excellent with experimental results for 0.5<Pr<1.0 and 5.10^5<Re_x<5.10^6; C = $0.0287Pr^{-0.4}$ and n=0.20.

Introducing the proposed correction for inclined surfaces:

$$St_{TurbExp} = \frac{0.0287Pr^{-0.4}Re_x^{-0.20}}{1+\frac{\beta}{5}} \quad (48)$$

Figure 7 shows the theoretical-experimental comparison for Stanton number in laminar regime, for β=1.0. The results are quite satisfactory for Prandtl numbers close to the unit, and deviate to high values of the Prandtl number, as expected.

Figure 8 presents theoretical and experimental data for turbulent regime, on smooth and rough surfaces, for the number of Pr=1.0. As expected, heat transfer on rough surfaces outweighs heat transfer to smooth surfaces, for the same Reynolds number.

The theoretical expression for determination of Stanton's number is given by, following application of empirical modification suggested by Kays and Crawford (1983):

$$St_{rug} = \frac{(Cf/2)_{rug}}{\left(\sqrt{(Cf/2)_{rug}}\,(13.2Pr-10.16)+Pr_t\right)(1.0+\frac{\beta}{5})} \quad (49)$$

In a completely rough flow, the molecular thermal conductivity remains as a significant variable, influence that can be established through the number of turbulent

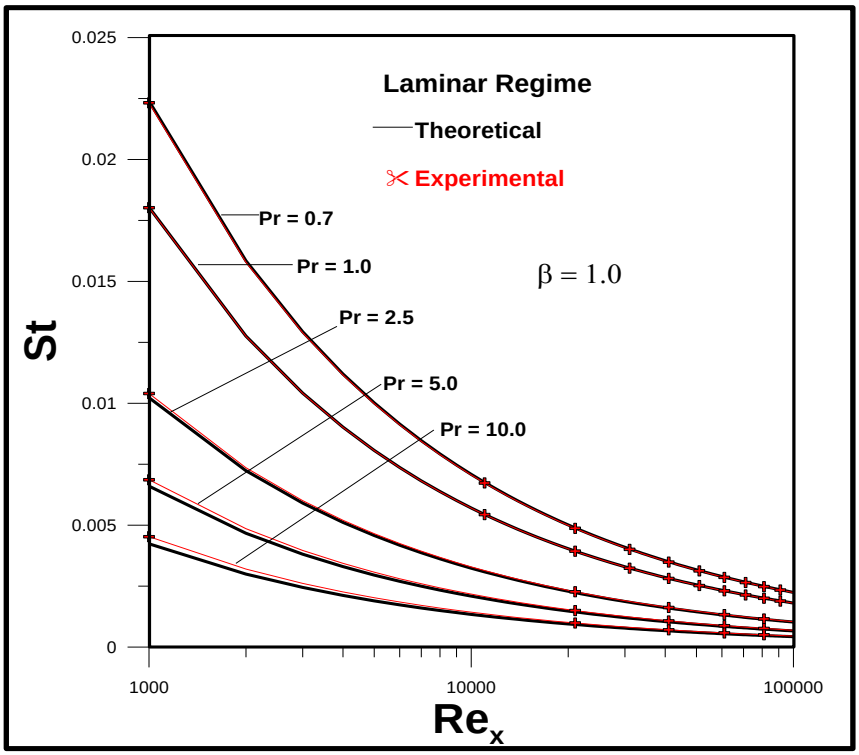

Figure 7. Stanton number (St) for laminar regime as a function of Reynolds number.

Prandtl, Pr_t. The turbulent Prandtl number can be considered, for gases, to be 0.9, which in fact represents an average value.

The equation for determination of experimental Stanton number, with the correction for the pressure gradient, is given by:

$$St_{Exp} = \frac{(\frac{Cf}{2})_{rug}}{(Pr_t + \sqrt{(\frac{Cf}{2})_{rug}}\Big/ St_k)(1+\frac{\beta}{5})} \quad (50)$$

$$St_k = {Re_k}^{-0.2} Pr^{-0.44} \quad (51)$$

Where St_k is a function of the roughness.

Figure 8 show that, for accelerated flow, the values approximate the result obtained for laminar flow, for smooth and rough surfaces. This effect is called laminarization of the boundary layer (Kays *et al.*, 1969) and demonstrates that the acceleration effect tends to cause a "retransmission" of the turbulent boundary layer to a pure laminar boundary layer. This is an effect associated with decompression of the boundary layer, where the roughness is immersed in the laminar sublayer. Table 2 shows the effect of the tendency for laminar flow in the numerical determination of the Stanton number.

Experimental results, with correction factor, obtained by Pimenta *et al*. (1975) and Kays and Crawford (1983) were used for comparison, Equation (50). The data were taken from the table of Pimenta (1975), where U=130.63 ft/s and without surface perspiration effect. The value of Ks is equal to 1.0 mm for all purposes in this analysis.

It is important to emphasize that there is experimental evidence that the shape factor tends to 1.47, for smooth surface and highly accelerated flows in completely turbulent flow. This shows that despite the tendency to the laminar regime, the flow remains turbulent because the value of the form factor for highly accelerated laminar flow is approximately 2.2, as presented through the results obtained in this work, Figures 9 and 10.

There is theoretical and experimental evidence that the detachment of the turbulent boundary layer is delayed in relation to the laminar boundary layer detachment. The numerical results presented through Figure 9 demonstrate that in fact this occurs. Note, Figure 10, that the smallest value for the parameter that establishes the pressure gradient is equal to $\beta = -0.19883768 \cong -0.200$, for laminar regime.

In fact, as the results of Figure 11 show, the dimensionless viscous stress passes through a local maximum point, close to $\beta = -0.2$, decreases asymptotically to approximately $\beta = -0.24$, where it becomes equal to zero, for turbulent regime on smooth surface.

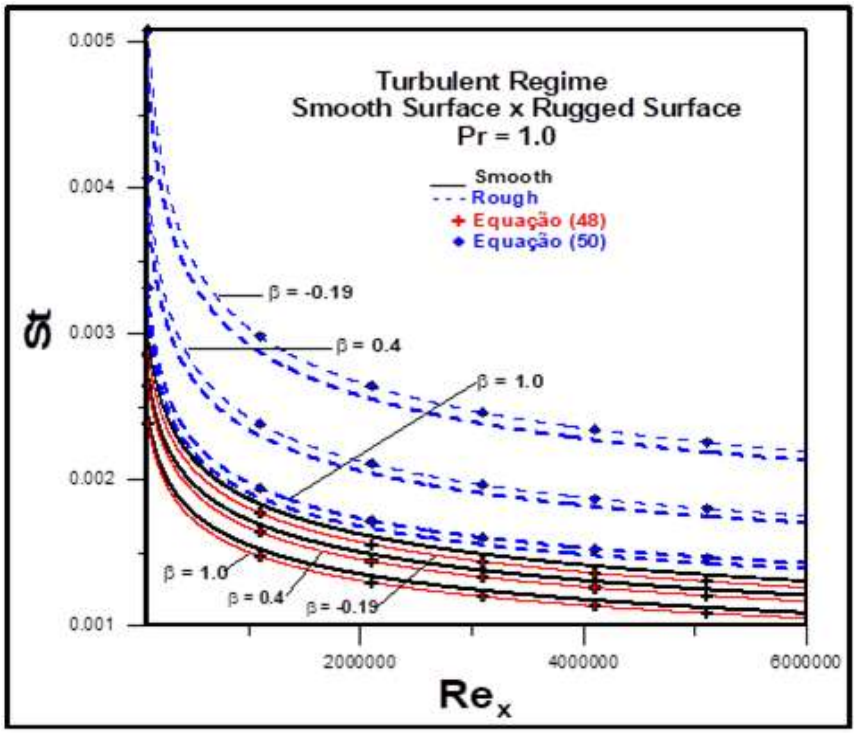

Figure 8. Theoretical-experimental comparisons for Stanton number (St) in turbulent regime, as a function of Reynolds number for smooth and rough surfaces.

Table 2. Stanton number (St) for turbulent regime in smooth and rough surfaces.

$R_e(x)$	$\beta = 0.0$		$\beta = 1.0$	
	Equation (48) Smooth	Equation (50) Rough	Equation (48) Smooth	Equation (50) Rough
1.01E5	2.864E-3	4.721E-3	2.387E-3	2.977E-3
2.01E5	2.496E-3	3.988E-3	2.080E-3	2.804E-3
4.01E5	2.174E-3	3.412E-3	1.812E-3	2.398E-3
6.01E5	2.005E-3	3.132E-3	1.671E-3	2.199E-3
8.01E5	1.9893E-3	2.953E-3	1.577E-3	2.073E-3
1.00E6	1.810E-3	2.824E-3	1.509E-3	1.983E-3
1.20E6	1.746E-3	2.726E-3	1.455E-3	1.913E-3
1.40E6	1.693E-3	2.646E-3	1.411E-3	1.857E-3
1.60E6	1.648E-3	2.580E-3	1.373E-3	1.810E-3
1.80E6	1.610E-3	2.524E-3	1.341E-3	1.770E-3
2.00E6	1.576E-3	2.475E-3	1.314E-3	1.736E-3

CONCLUSIONS

The analysis, for flow and heat transfer in laminar regime and turbulent regime, on smooth and rough inclined surface, includes theoretical aspects, experimental results and empirical correlations. An extensive review of procedures associated to the boundary layer similarity method, used for solution of nonlinear equations systems, was presented.

In a turbulent regime, through the integral analysis of the momentum, the equations were first obtained for null pressure gradient and extended through a correction factor, for a wide range of the pressure gradient parameter.

The main result of the present work is associated with the fact that it is possible to obtain empirical solutions compatible with analytical solutions for laminar and turbulent flow in the whole range of values for the pressure parameter, β, considered in the analysis. This result allows us to use reliable solutions for numerous practical problems without having to solve the system of nonlinear equations, which is the main source of

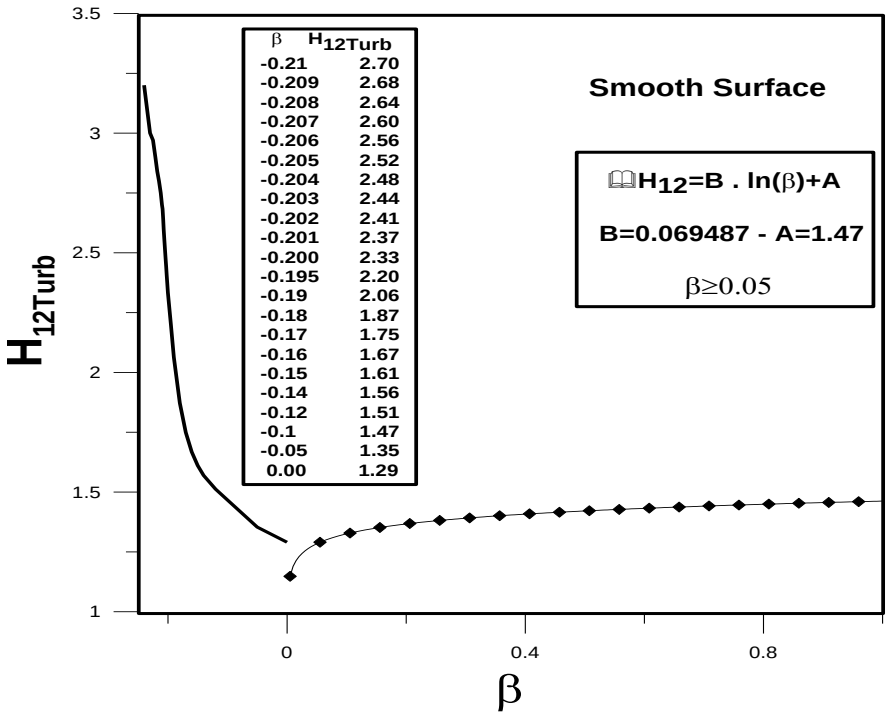

Figure 9. Shape Factor (H_{12}) for turbulent regimen on smooth surface.

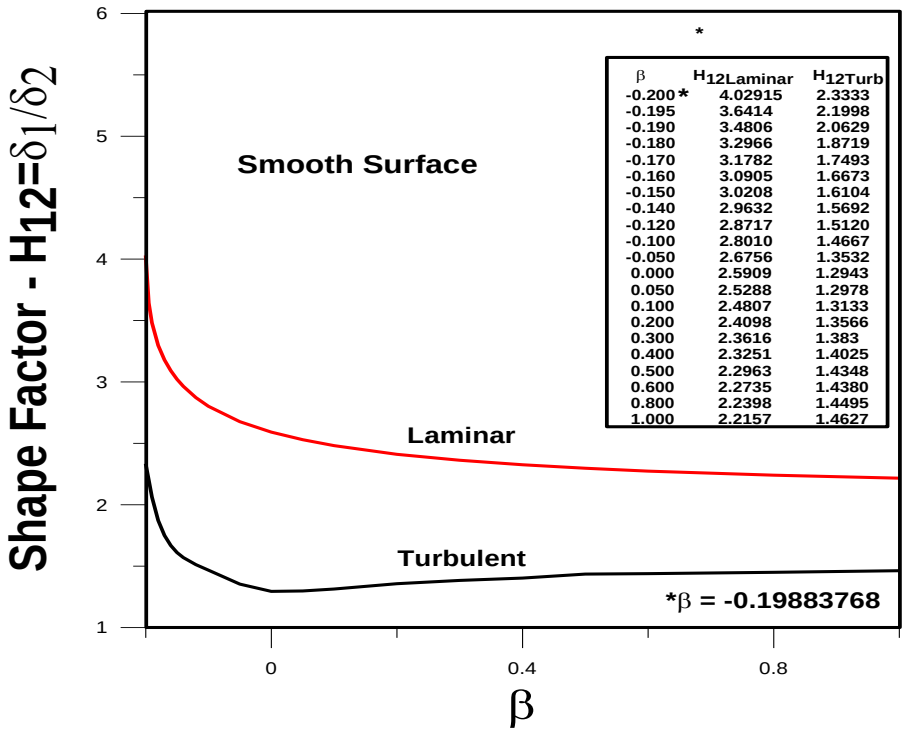

Figure 10. Shape factors (H_{12}) for laminar and turbulent regimes on smooth surfaces.

difficulties in the analysis performed.

As a motivation for the development of future works, it can be stated that problems associated to the determination of micrometeorological parameters, through the

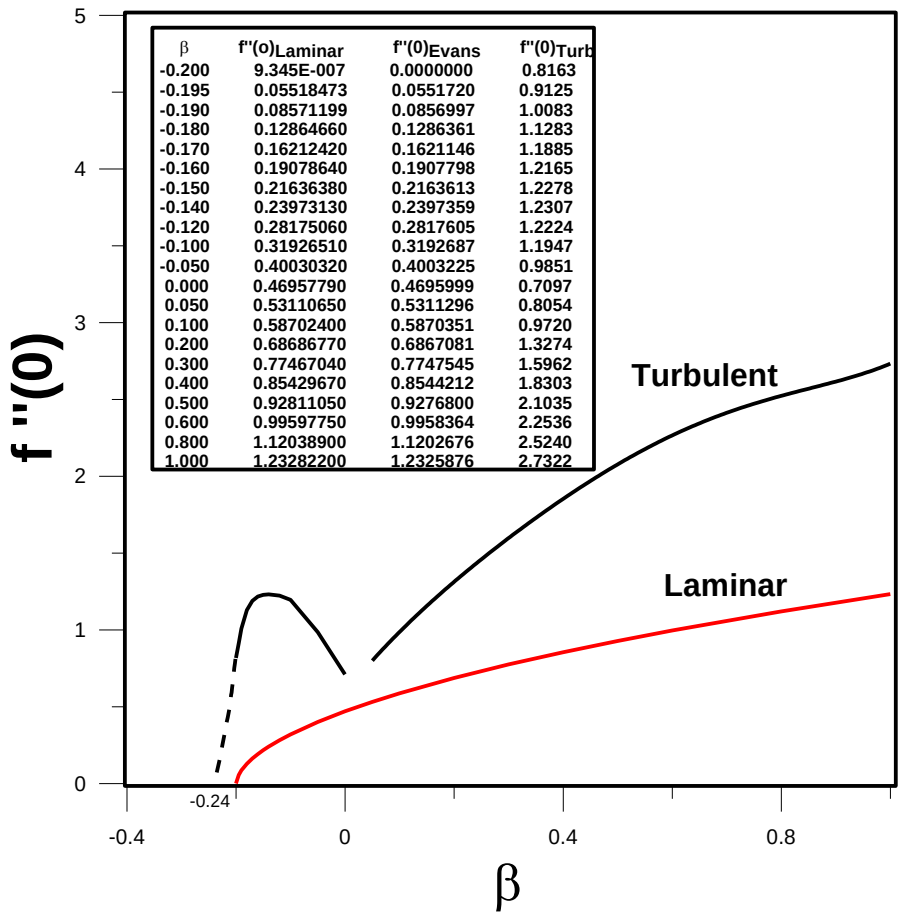

Figure 11. Dimensionless viscous surface tension (f'') for laminar and turbulent regimes.

Monin-Obukov similarity theory, in inclined rugged surface, can be solved in an approximate way through the application of the analysis performed in this work.

REFERENCES

Abbasi M, Nava GH, Petroudi IM (2014). "Analytic Solution of Hydrodynamic and Thermal Boundary Layer over a Flat Plate in a Uniform Stream of a Fluid with Convective Surface Boundary Condition". Indian J. Sci. Res.1 (2):241-247.

Bhattacharyya K, Uddin MS, Layek GC (2016). "Exact Solution for Thermal Boundary Layer in Casson Fluid Flow over a Permeable Shrinking Sheet with Variable Wall Temperature and Thermal Radiation". Alexandria Eng. J. 55:1703-1712.

Blasius H (1908). "Boundary layers in liquids with low friction". Z. Math, und Phys. 56:1. (In German).

Bognar G, Hriczó K (2011). "Similarity Solutions a Thermal Boundary Layer Models of a non-Newtonian Fluid with a Convective Surface Boundary Condition". Acta Polytechnica Hungarica 8:6.

Castilho L (1997). "Similarity Analyses of Turbulent Boundary Layer". A Dissertation Submitted in a Partial Requirement for the Degree of Doctor of Philosophy, State University of Buffalo.

Evans HL (1968). "Laminar Boundary-Layer-Theory". Addison-wesley Publishing company.

Grapher 5.01.15.0 (2004). Golden Software, Inc.

Falkner VM, Skan SW (1930). "Some approximate solutions of the boundary layer equations"**.** British Aero. Res. Council, Reports and Memoranda. p. 1314.

Falkner VM, Skan SW (1931). LXXXV Solutions of the boundary-layer equations. Phil. Mag. 12(7):865-896.

Hager WH (2003). "Blasius: A Life in Research and Education". Experiments in Fluids, 34:566-571.

Kays WM, Crawford ME (1983). "Convective Heat and Mass Transfer". Tata McGraw-Hill Publishing Co. Ltd, New Delhi.

Kays WM, Moffat RJ, Thiebhr HW (1969). "Heat Transfer to the Highly Accelerated Turbulent Boundary Layer with and without Mass Addition". Report Nº HMT-6.

Microsoft Fortran Power Station Version 4.0 (1995). Microsoft Corporation.

Sobamowo MG, Yinusa AA, Oluwo AA, Alozie SI (2018). "Finite element analysis of flow and heat transfer of dissipative Casson-Carreau nanofluid over a stretching sheet embedded in a porous medium". Aeronautics and Aerospace Open Access J. Res. Article 2:5.

Nazeer M, Ali N, Tariq J (2017) "Numerical simulation of MHD flow of micropolar fluid inside a porous inclined cavity with uniform an non-uniform heated bottom-wall". Can. J. Phys. 96(6):576-593.

Myers TG (2010). "An Approximate Solution Method for Boundary Layer Flow of a Power Law Fluid over a Flat Plate". Int. J. Het and Mass Transfer, 53:2337-2346.

Khan NA, Khan S, Ara A (2017) "Flow of micro polar fluid over an off centered rotating disk with modified Darcy's law". Propulsion Power Res. 6(4):285-295.

Ali N, Nazeer M, Tariq J, Mudassar R (2019). "Finite element analysis of bi-viscosity fluid enclosed in a triangular cavity under thermal and magnetic effects". The Eur. Phys. J. 134:2.

Nogueira É, Soares MVF (2018). "Flat plate boundary layer: revisiting the Similarity Method". Cadernos UniFOA, Volta Redonda, 37:15-31.

Oderinu RA (2014). “Shooting Method via Taylor Series for Solving Two Point Boundary Value Problem on an Infinite Interval”. Gen. Math. Notes 24(1):74-83.
Pimenta MM, Moffat RJ, Kays WM (1975). “The Turbulent Boundary Layer: An experimental Study of the Transport of Momentum and Heat Transfer with Effects of Roughness”. Report Nº HMT-21.
Puttkammer PP (2013). “Boundary Layer over a Flat Plate”. BSc Report, University of Twente, Enschede.
Rabari MF, Hamzehnezhad A, Akbari VM, Ganji DD (2017) “Heat transfer and fluid flow of blood with nanoparticles through porous vessels in a magnetic field: A quasi-one-dimensional analytical approach”. Math. Biosci. 283:38-47.
Rahman MM (2011). “Locally Similar Solutions for a Hydromagnetic and Thermal Slip Flow Boundary Layers over a Flat Plate with Variable Fluid Properties and Convective Surface Boundary Condition”. Meccanica, 46:1127-1143. doi: 10.1007/s11012-010-9372-2.
Aziz RC, Hashim I, Abbasbandy S (2018). “Flow and Heat Transfer in a Nanofluid Thin Film over an Unsteady Stretching Sheet”. Sains Malaysiana 47(7):1599-1605.
Schultz-Grunow F (1941): NA TM-986, Washington.
Schlichting H (1968). McGraw-Hill Book Company, New York.
Sheikhzadeh MM, Abbaszadeh M (2018). “Analytical study of flow field and heat transfer of a non-Newtonian fluid in an axisymmetric channel with a permeable wall”. J. Comput. Appl. Res. Mech. Eng. 7(2):161-173.
Simpson RL (1989). “Turbulent Boundary-Layer Separation”. Ann. Rev. Fluid Mech, 21:205-340.
Silva FAP (1990). "Boundary Layer Theory: Notes of Classes”. Mechanical Engineering Program. (In Portuguese).
Spalding DB, Pun WM (1962). “A Review of Methods for Predicting Heat-Transfer Coefficients for Laminar Uniform-Property Boundary Layers Flows”. Int. J. Heat Mass Transf. 5:239-249. Pergamon Press.
Stemmer C (2010). “Boundary Layer Theory: Falkner-Scan Solution (Flat-Plate Boundary Layer with Pressure Gradients)”. Lehrstuhf für Aerodynamik, Tecnische Universität Münchem, Boundary Layer Theory, GIST.
Stull RB (1988). “An Introduction on Boundary Layer Meteorology”. Atmospheric Sciences Library, Kluwer Academic Publishers, London.
Tannehill JC, Anderson DA, Plecher RH (1997). “Computational Fluid Mechanics and Heat Transfer”. Second Edition, Taylor & Francis.